

High Resolution X-Ray: A Reliable Approach for Quantifying Osteoporosis in a Rodent Model

Omar Velasco,¹⁻³ Aaron W. James,^{1,2,4} Greg Asatrian,¹ Mark Ajalat,^{1,2} Tyler Pritchard,^{1,2} Siyouneh Novshadian,¹ Anu Murthy,¹ Georgina Bayani,^{1,2} Xinli Zhang,^{1,2} Kang Ting,^{1,2} and Chia Soo^{2,5}

Abstract

Osteoporosis is the most common metabolic disease of bone, resulting in significant worldwide morbidity. Currently, there are insufficient imaging modalities available to evaluate osteoporotic bones in small animal models. Here, we demonstrate the feasibility of using high resolution X-ray imaging as a comparable measure of bone degeneration to dual-energy X-ray absorptiometry (DXA) in an osteoporosis rodent model. At week 0, animals underwent either an ovariectomy (OVX) or sham procedure (SHAM). DXA analysis was performed weekly to confirm and compare the bone degenerative changes induced by OVX. A comparison using high resolution X-ray imaging (Faxitron[®]) was then performed postmortem due to need of soft tissue removal. Two regions of interest (ROIs) were utilized: the distal third of the femur and the lumbar spine (L4/L5). It was observed that SHAM animals maintained a relatively constant bone mineral density (BMD), in comparison to OVX animals, whereby a significant decrease in BMD was appreciated. Post mortem X-ray scans were performed and converted to 8-bit color and quantified. A high level of agreement with DXA quantifications was observed with X-ray quantifications, and a significant correlation between the radiopacity, visualized by color distributions, and the DXA BMD values between animal groups was evident. Our study demonstrates the applicability of high resolution X-ray imaging both qualitatively and quantitatively as a reliable approach for quantifying osteoporosis in rodent osteoporotic models. With DXA being a highly user dependent modality, our technique is a unique secondary methodology to verify DXA findings and minimize inter-observer variability.

Key words: ovariectomy; osteoporosis; DXA; dual-energy X-ray absorptiometry; X-ray

Introduction

AN ESTIMATED 200 MILLION individuals worldwide are afflicted by osteoporosis, a number that is only increasing with the growing size of the elderly population.¹ Osteoporosis is a disease defined by a bone mineral density (BMD) of 2.5 standard deviations below the mean peak bone mass (typically measured by dual-energy X-ray absorptiometry [DXA]).² In order to understand the pathoetiology and improve treatment for this common disease process, there is an immense need for research using small animal models.

The ovariectomy (OVX)-induced osteoporotic rodent model has frequently been used for the study of bone resorption seen in osteoporotic humans.³ The simulated postmenopausal cancellous bone loss in mice and rats occurs for a

short period while the trabecular bone volume remains lower for several months.⁴ Because of these bone level trends, analyzing the benefit of bone therapies requires proper time planning.⁴ Specifically, experimental design requires periodic DXA imaging, spanning four to six weeks post-OVX in order to measure bone mineral content of cancellous bone.

DXA is the current gold standard for osteoporosis confirmation, as it is simple, inexpensive, noninvasive, and exposes the patient to low radiation, thus minimizing the risk of tumorigenesis.^{5,6} Further, DXA scans can be repeatedly performed on the same patient over a period of time to track changes in bone density. DXA is commonly used to analyze the whole body, spine, hip, femur, and skeletal tissue.⁵ Although, a full body DXA image in humans offers a profile

¹Dental and Craniofacial Research Institute and Section of Orthodontics, School of Dentistry; ²Department of Orthopaedic Surgery and the Orthopaedic Hospital Research Center, UCLA and Orthopaedic Hospital; ⁴Department of Pathology and Laboratory Medicine; ⁵Division of Plastic and Reconstructive Surgery, Department of Surgery, David Geffen School of Medicine; University of California, Los Angeles, California.

³Department of Surgery, University of Maryland Medical Center, Baltimore, Maryland.

of the overall bone composition, spine and hip DXA imaging provide potential fracture assessment and continue to be the most commonly imaged regions.⁷ In small animal models, accessibility of a DXA machine and cumbersome calibration for BMD analysis make high resolution radiography an attractive alternative.

In this study, we sought to compare two imaging modalities for use in monitoring of BMD in mouse OVX-induced osteoporosis: DXA and high resolution X-ray imaging. All quantification of BMD in rodents (mice) focuses in the region of interest in osteoporosis—distal femur and lumbar vertebrae. Specifically, the distal femur is reported to undergo a decrease in trabecular bone volume early and throughout their life in an age dependent fashion.^{8–11}

Materials and Methods

Ovariectomy

All animal experiments received University of California, Los Angeles (UCLA) Chancellor's Animal Research Committee approval prior to being performed. Surgery was performed on 12- to 14-week-old B6 mice ($n=6$ per surgical group). The surgical site was clipped and aseptically prepped using povidone-iodine alternated with isopropyl alcohol in the standard fashion. Each mouse was placed in a ventral recumbency position, followed with draping of the lower dorsal spinal region. Starting from the caudal edge of the rib cage, a 3cm dorsal midline skin incision was extended to the tail base using a No. 10 scalpel blade. A 2–3 mm incision was made along the dorsal midline. Once the subcutaneous tissue was dissected, bilateral 1 cm vertical incisions were made into the lumbodorsal muscle. Kelly forceps were used to exteriorize the ovary and oviduct while entirely remaining in the retroperitoneal space. Then, a hemostat was placed onto the uterine vasculature for the excision of the ovaries near the distal segments of the oviducts. Finally, the hemostat was released and the muscle and skin were sutured with 5-0 vicryl. Similarly, the sham-operated group (SHAM) ($n=6$), underwent all of the steps mentioned above, excluding excision of distal segments of the oviducts and ovaries.

Harvest of femur and lumbar vertebrae

Animals were sacrificed 8 weeks following surgery and left and right femurs and lower lumbar vertebrae (L4–L6) were

harvested. Specifically, the removal of the femurs required detachment from the pelvis and tibia. Vertebral removal of the lumbar region (L1–L6) required transection caudal to thorax and at the base of the tail. Next, the listed bony structures underwent meticulous soft tissue removal before fixation in 70% ethanol solution at 4°C for at least 48 hours.

Dual-energy X-ray absorptiometry measurement

All DXA measurement was performed using a GE Lunar Prodigy Advanced System (GE Healthcare; Milwaukee, WI) using auto exposure for scanning. Data collected was analyzed by Encore 2007 Small Animal software (version 11.20.068). Before measuring the bone mineral density of the mice, the DXA machine was calibrated per manufacturer's instruction protocol. Measurements were attained by positioning the mice in prone position with knee flexed and extended hips. After isoflurane anesthesia (4%–5% for induction, 1.5%–2% for maintenance), the mice were then laid flat in a prone position on the DXA table. The mice extremities were pointing to the four table corners with the tail in a u-shape ending near the left upper extremity. Next, the regions of interest (ROIs) (distal femur, lower lumbar vertebrae) were measured in a duplicate to ensure no significant variance (Fig. 1A).

High resolution X-ray (Faxitron®) imaging and processing

All radiographs were performed using a Faxitron® LX-60 Cabinet radiography system with variable kV point projection X-ray source and digital image system (Qados, Cross Technologies plc, Berkshire, United Kingdom). A polypropylene sample is utilized to calibrate the high resolution X-ray machine. Calibration is achieved by performing four flat dark field images. A specific time (15 seconds) and voltage (26 kV) high resolution setting are selected and saved for all subsequent images, as described by Bassett et al.¹² Samples were loaded into the upper slot at 5× magnification before the following parameters were selected for exposure and imaging: contrast assist, auto exposure control, sharpen assist toggles, and auto level. Then the femurs and lumbar vertebrae were oriented into their respective positions. All femurs were positioned supine with the proximal portion in the upper pole and the posterior shaft in direct contact with the undersurface. This configuration ensures the two-dimensional radiograph and the grayscale pixels within the image are identical when further analysis is undertaken. Lastly, a digital imaging and communications in medicine (DICOM) file (16,383 gray

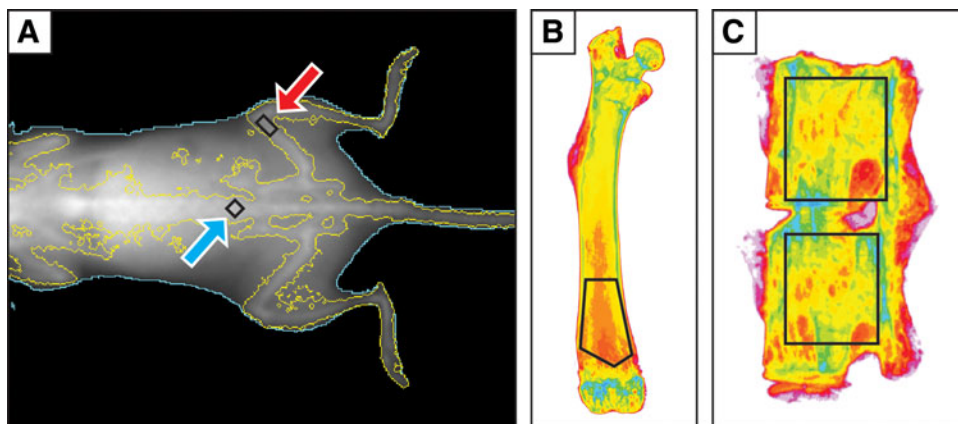


FIG. 1. (A) Two regions of interest were drawn for dual-energy X-ray absorptiometry (DXA) scans: lumbar spine (blue arrow) and distal femur (red arrow). (B, C) After Faxitron scans were performed and colorized, regions of interest were selected for in the distal femur and lumbar spine respectively.

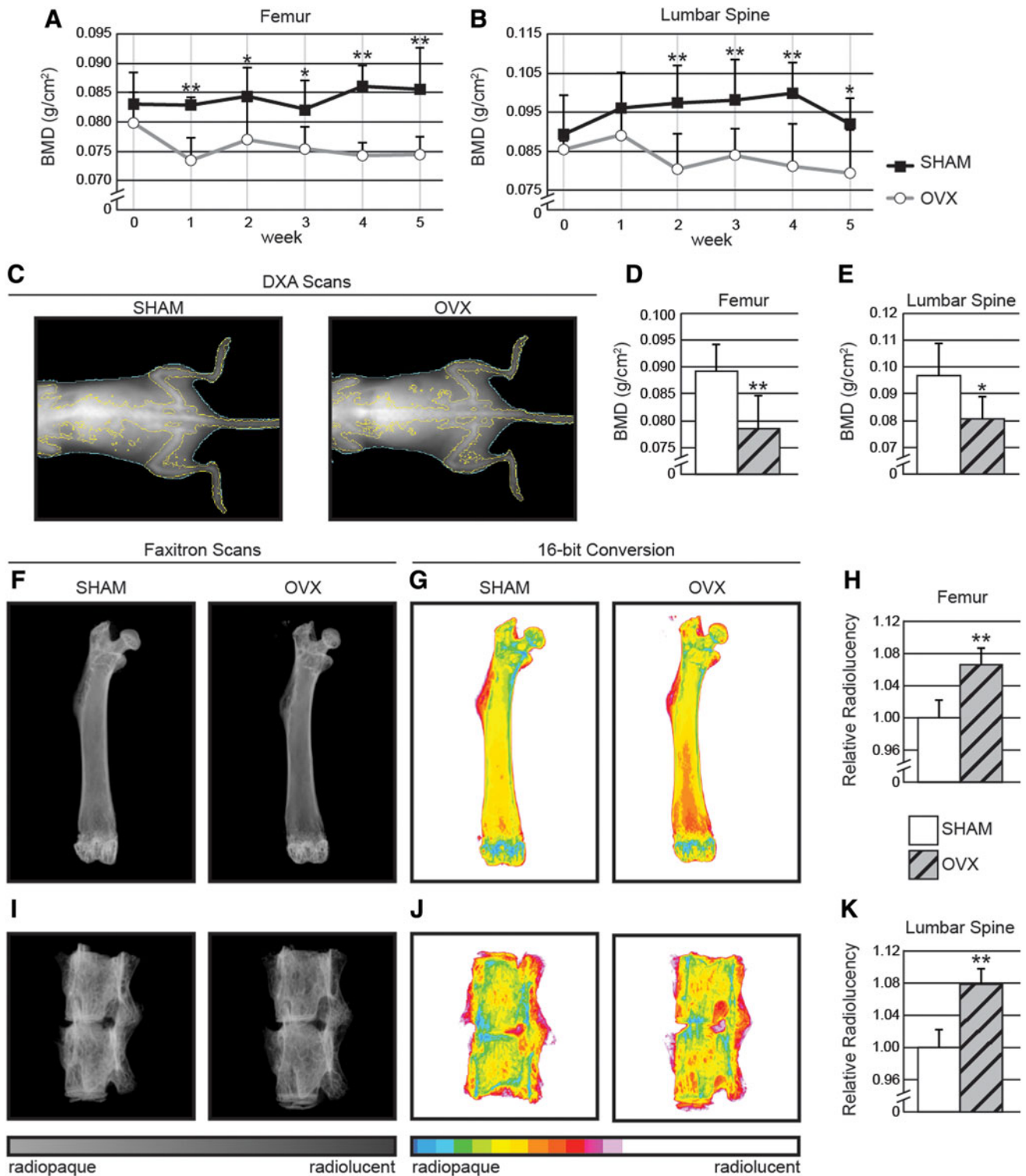


FIG. 2. DXA scans of (A) distal femur and (B) lumbar spine exhibit a significant and gradual decrease in bone mineral density (BMD) in the ovariectomized (OVX) animals when compared with control. Qualitative (C) and quantitative analysis of (D, E) OVX animals revealed significant decreases in BMD by 1–2 weeks in both the femur and lumbar vertebrae regions of interest respectively. (F) Postmortem Faxitron scans of animals’ femurs were next performed and converted to (G) 16-bit color. (H) Quantifications for relative radiolucency in the femur. (I, J, K) Identical protocol was performed for L5–L6 vertebrae. **p* < 0.05; ***p* < 0.01.

levels) was generated with the corresponding histogram and grayscale pixel distribution. The gray level values the maximum and minimum generated from the histogram. Grayscale stretch procedure was finally performed with the steel and polyester standard for the modal gray levels¹³ so that the image could be inverted and converted into an 8-bit tagged image file format (TIFF) file (256 gray levels) (Fig. 1B,C). Steel (255 gray level) and polyester (0 gray level) are denoted with their respective values.

Determination of bone pseudo-colored images and relative mineral content

Each of the stretched 8-bit grayscale TIFF images opened with a 16-color scale. Using Adobe Photoshop, the TIFF file was edited with the brush tool to remove all remaining soft tissue. Next, the opened TIFF file under the custom-histogram and the frequency distribution of pixel number were extrapolated using 16 equal gray level divisions in Microsoft Excel. A comparative analysis of the relative gray level distributions was then performed between the OVX and SHAM group.

Statistical analysis

All quantifications were reported as mean values with respective standard deviations. Statistical analysis was performed using an appropriate Student's *t*-test. Based on the grayscale images, the OVX and SHAM-operated groups were compared for differences in bone mineral density in DXA scans and the cumulative frequency distribution in Faxitron scans; $p < 0.05$ and $p < 0.01$ were considered statistically significant.

Results

Quantitative analysis of BMD by DXA

DXA scans were performed weekly to confirm the induction of osteoporosis. Bone mineral density (BMD) measurements were obtained from scans at two ROIs: the distal one-third of the femur and the lumbar spine (L4–L5). SHAM-operated animals maintained relatively constant BMD, ranging between 98–113% of their initial values. In contrast, a significant decrease was observed by 4 weeks post-OVX in the distal femur (Fig. 2A) and by 2 weeks post-OVX in the lumbar spine (Fig. 2B). OVX-induced osteoporosis was confirmed at 5 weeks postoperative in OVX animals by a 7%–8% decrease, compared with preoperative BMD, measured at both the distal femur and lumbar spine ROIs, consistent with the previous studies.^{8–10}

Quantitative analysis of relative bone radiopacity by high resolution X-ray

DXA scans between treatments groups were next compared qualitatively with high resolution X-ray scans. The final DXA timepoint (8 weeks) performed on the day of euthanasia was compared with postmortem femur and lumbar spine. Qualitative analysis of X-ray images showed that SHAM animals exhibited a more dense bone composition, when compared to OVX animals (Fig. 2C). DXA values revealed a 12% and 16.6% lower BMD in the distal femur and lumbar spine, respectively, when OVX animals were compared with those with SHAM treatment (Fig. 2D, E).

Animals were next sacrificed, and samples were harvested for X-ray analysis. Increased radiolucency in the distal femoral region was observed in OVX animals (Fig. 2F), confirming the previously observed decrease in BMD by DXA scans. Next, DICOM files were converted to a pseudo-color 16-bit TIFF image using ImageJ software to give a visual representation of the relative gray level distributions. When quantified, it was confirmed that there was, in fact, a significant correlation between the color distributions and the DXA BMD values between animal groups. OVX animals were observed to possess a significantly more radiolucent bone composition in the distal femur, when compared with SHAM treated animals (Fig. 2G). To assess femurs quantitatively, ROIs were drawn in the cancellous bone of the distal third of the femur (Fig. 1B) and mean 16-color bin scale values were obtained. It was observed that OVX animals exhibited a 6.5% increase in relative radiolucency when compared with SHAM animals (Fig. 2H). Next, similar conversions to 16-bit color were performed on L4–L5 vertebral bodies (Fig. 1C, and 2I, J). Again, we observed an increase (7.7%) in relative radiolucency when OVX animals were compared with SHAM treatment (Fig. 2K). In summary, X-ray DICOM images and quantification presented similar results to DXA scans, exhibiting significant increases in radiolucency both in the distal femoral region and lumbar spine in OVX-treated samples, correlating with lower BMD as calculated by DXA.

Discussion

In this study, we sought to compare the reliability of using high resolution X-ray as a viable secondary means to DXA in the setting of osteoporotic bone loss. It was observed that similar and significant trends exist between DXA and X-ray at both the distal femur and lumbar spine regions of interest. The SHAM-operated animals maintained a relatively constant bone mineral density. In the OVX treatment group, a significant decrease was observed at 2 weeks post-OVX in the lumbar spinal region, and at 4 weeks post-OVX in the distal femoral region. When quantified using mean histogram values, it was confirmed that there was a significant correlation between the color distributions and the DXA BMD values between animal groups. Thus, we can safely conclude that X-ray can be used as a relatively inexpensive and reliable assay to confirm DXA findings.

Although rodent DXA are efficient and can be performed numerously on the same animal, high user dependency exists.¹⁴ This interobserver variability can be attributable to a variety of factors including differences in animal positioning, consequently resulting in variable soft tissue imposition and inconsistent radiodensity measurements.¹⁵ As high resolution X-ray imaging was shown to measure BMD in rodents,² and to detect similar bone changes in the selected ROIs, it is proving as a potential comparable modality for measuring BMD in an osteoporotic model. Further, other investigators have also shown the efficacy of X-ray imaging as a modality to monitor bone density.^{16,17} Their methods of quantification, however, consist of cortical width measurements¹⁶ and assessment of bone diameter.¹⁷ In our study, all high resolution X-ray calibration and image analysis was performed as described by Bassett et al.¹² to quantify radiopacity. This study characterizes an imaging modality to measure the cancellous bone changes in a

well-accepted osteoporotic disease model. Compared with the gold standard, DXA, high resolution X-Ray imaging detected similar bone changes in the selected ROIs.

The OVX-induced osteoporotic rodent bones utilize an anterior-posterior view of the distal femur and lower lumbar vertebrae (L4–L6) which were preemptively selected based on the expected disease affected areas seen in human osteoporosis.^{2,18,19} Often, the trabecular bone in these areas undergoes intense remodeling with impact over time.¹⁸ Once cancellous bone degeneration increases between 30 and 35 years of age,¹⁸ the femur and spine become subject to osteoporotic fracture sites. The reproducible measuring sites, as in the ROI in this study, have decreasing trabecular fractional bone volume.⁸ In the rodent model, these areas tend to have weaker bone spicule formation and resorption and a balance between the two during the estrogen deficient state. OVX-induced osteoporotic mice have more active bone sites that undergo intense remodeling and begin to be replaced with weaker bone.¹⁹ Appropriate timing was imperative to yield a significant quantitative cancellous bone changes when using high resolution X-ray.^{8–11} Furthermore, the bone ROIs are quintessential to measure the disease-focused approach using high resolution X-ray.

Finally, our study has a number of limitations, which could be expanded upon in future reports. First, a major drawback to our study is the need to dissect limbs in order to accurately image samples with X-ray. As this is not clinically relevant, future studies should seek to assess whether a modified X-ray imaging and quantification protocol can be applied, such as to monitor changes in bone opacity over a period of time. Soft tissue may, however, pose as a confounding variable and again result in the inter-observer variability seen in DXA.^{14,16,17} Subsequent studies must also confirm these findings in a large animal model. If similar trends are observed, these findings can extrapolated and potentially used in a clinical setting, utilizing X-ray imaging as a viable confirmatory modality to diagnose osteopenia and osteoporosis.

In conclusion, our study demonstrates the applicability of using high resolution X-ray imaging quantitatively as a secondary methodology to verify DXA findings, allowing reliable BMD results by eliminating the interobserver variability in DXA usage.

Author Disclosure Statement

The authors have no disclosures or conflicts of interest, as no competing financial interests exist.

References

1. Reginster JY, Burlet N. Osteoporosis: a still increasing prevalence. *Bone*. 2006;38:S4–S9.
2. Assessment of fracture risk and its application to screening for postmenopausal osteoporosis. Report of a WHO Study Group. *World Health Organ Tech Rep Ser*. 1994;843:1–129.
3. Namkung-Matthai H, Appleyard R, Jansen J, et al. Osteoporosis influences the early period of fracture healing in a rat osteoporotic model. *Bone*. 2001;28:80–86.
4. Turner AS. Animal models of osteoporosis—necessity and limitations. *Eur Cell Mater*. 2001;1:66–81.
5. Larkin A, Sheahan N, O'Connor U, et al. QA/acceptance testing of DEXA X-ray systems used in bone mineral densitometry. *Radiat Prot Dosimetry*. 2008;129:279–283.

6. Kallai I, Mizrahi O, Tawackoli W, et al. Microcomputed tomography-based structural analysis of various bone tissue regeneration models. *Nat Protoc*. 2011;6:105–110.
7. Johnson LC, Johnson RW, Munoz SA, et al. Longitudinal live animal micro-CT allows for quantitative analysis of tumor-induced bone destruction. *Bone*. 2011;48:141–151.
8. Willingham MD, Brodt MD, Lee KL, et al. Age-related changes in bone structure and strength in female and male BALB/c mice. *Calcif Tissue Int*. 2010;86:470–483.
9. Glatt V, Canalis E, Stadmeier L, et al. Age-related changes in trabecular architecture differ in female and male C57BL/6J mice. *J Bone Miner Res*. 2007;22:1197–1207.
10. Ferguson VL, Ayers RA, Bateman TA, et al. Bone development and age-related bone loss in male C57BL/6J mice. *Bone*. 2003;33:387–398.
11. Tezval M, Stuermer EK, Schmisch S, et al. Improvement of trochanteric bone quality in an osteoporosis model after short-term treatment with parathyroid hormone: a new mechanical test for trochanteric region of rat femur. *Osteoporos Int*. 2010;21:251–261.
12. Bassett JH, van der Spek A, Gogakos A, et al. Quantitative X-ray imaging of rodent bone by Faxitron. *Methods Mol Biol*. 2012;816:499–506.
13. Manninen AH. Very-low-carbohydrate diets and lean body mass. *Obes Rev*. 2006;7:297; author reply 297–298.
14. Rozenberg S, Vandromme J, Neve J, et al. Precision and accuracy of in vivo bone mineral measurement in rats using dual-energy X-ray absorptiometry. *Osteoporos Int*. 1995;5:47–53.
15. Javed F, Yu W, Thornton J, et al. Effect of fat on measurement of bone mineral density. *Int J Body Compos Res*. 2009;7:37–40.
16. Mijares D, Kulkarni A, Lewis K, et al. Oral bone loss induced by mineral deficiency in a rat model: effect of a synthetic bone mineral (SBM) preparation. *Arch Oral Biol*. 2012;57:1264–1273.
17. Beauchesne PD. Age-related cortical bone maintenance and loss in an Imperial Roman population. *J Osteoarchaeol*. 2014;24:15–30.
18. Prevention and management of osteoporosis. *World Health Organ Tech Rep Ser*. 2003;921:1–164, back cover.
19. Old JL, Calvert M. Vertebral compression fractures in the elderly. *Am Fam Physician*. 2004;69:111–116.

Address correspondence to:

Chia Soo, MD, FACS
 Department of Orthopaedic Surgery
 University of California, Los Angeles
 675 Charles E Young Drive South, MRL 2641A
 Los Angeles, CA 90095

E-mail: bsoo@ucla.edu

Abbreviations Used

BMD = bone mineral density
 DICOM = digital imaging and communications
 in medicine
 DXA = dual-energy X-ray absorptiometry
 OVX = ovariectomy
 ROI = region of interest
 TIFF = tagged image file format